A Review of Geometrical Interface Properties for 3D Front-Tracking Methods

Désir-André Koffi Bi(✉), Mathilde Tavares, Éric Chénier, and Stéphane Vincent

Univ. Gustave Eiffel, CNRS, MSME UMR 8208, 77454 Marne-la-Vallée, France
desir-andre.koffibi@u-pem.fr

Abstract. Modeling and simulating multiphase flows still remain an exciting and stimulating scientific challenge. Many approaches were developed to describe the topological evolution of the interface. This paper remains in the domain of the Front-Tracking method [8,10], in which, in addition to the use of an Eulerian mesh to solve the Navier-Stokes equations, a Lagrangian interfacial mesh of surface elements (triangles in 3D) explicitly describes the evolution of the interface. Whatever the method used, getting the interfacial capillary, mass or energy transfers is crucial for the study of multiphase flows. A comparison is done between different techniques [7,10] used to get the geometrical properties of the 3D front-tracking objects, such as the surface tension forces, mean curvatures and normal vectors, which are essential for the modeling and understanding of multiphase flows.

Keywords: Front-tracking · Multiphase flow · Surface tension · Curvature

1 Introduction

The numerical simulation and modeling of multiphase flows have been of great interest these last two decades. It has a wide range of involvements in our daily life, whether in chemical engineering, material design, energy field or propelling, with boiling crisis, combustion in motors, atomization, surface coating, to cite but a few. Different approaches are used to take into account the surface tension forces. In the Direct Numerical Simulation (DNS) of multiphase flows, unstructured meshes are usually used for discretization [2]. Each phase is resolved independently, and the junction at the interface is satisfied through jump conditions [3], including the surface tension forces. In the case of the One-Fluid model, contrary to the previous one, a structured mesh is often used to solve the conservation equations in the entire domain. The surface tension forces $\mathbf{F}_{st}$ are included in the Navier-Stokes equations. One way to estimate them is using the Continuum Surface Force (CSF) proposed by Brackbill *et al.* [1]. But

M. Deville et al. (Eds.): TI 2018, NNFM 149, pp. 144–149, 2021.
https://doi.org/10.1007/978-3-030-65820-5_15

whatever the method employed, the mean curvature κ and the unit normal vector $\mathbf{n}$ must be accurately evaluated, for they are essential geometrical properties for the study of multiphase flows and interfacial transfers. In the case of 3D front-tracking methods, four approximations are presented and compared to get those surfaces properties.

2 Geometrical Interface Properties

Four approaches to get the geometrical properties of the interface, namely the mean curvature κ and the unit normal vector $\mathbf{n}$, are shown below, knowing the triangular interface mesh (vertices positions and mesh connectivity). They can be gathered into two groups.

2.1 The Meyer et al. Approach

The Meyer approach is based on a discrete formulation of the Laplace-Beltrami operator [7]. The curvature and the normal vector are obtained through a linear combination of the $\mathcal{N}_i$ edges sharing the same vertex $\mathbf{x_i}$.

$$\mathbf{K}(\mathbf{x}_i) = \frac{1}{2\mathcal{A}_{mixed}} \sum_{j=1}^{\mathcal{N}_i} (\cot \alpha_{ij} + \cot \beta_{ij})(\mathbf{x}_i - \mathbf{x}_j) = 2\kappa \mathbf{n} \tag{1}$$

where α_{ij} and β_{ij} are the angles facing the edge $[\mathbf{x_i x_j}]$, and $\mathbf{K}$ is the Laplace-Beltrami operator, which is basically a Laplacian acting on the surface (see Fig. 1b). Two variants can be differentiated based on the construction of the area $\mathcal{A}_{mixed}$: the Standard Meyer Method [7] and the Barycentric Meyer Method [4]. In both cases, when the triangle is acute, the Voronoi area is used. If the triangle is obtuse, either the middle of the edge opposite to the obtuse angle (Standard Meyer Method), or the centroid (Barycentric Meyer Method) is employed to construct $\mathcal{A}_{mixed}$.

2.2 The Frenet Approach

The Frenet approach is used in the works by Shin and Juric [8], as well as in those by Tryggvason *et al.* [10]. Evaluated on an element (line in 2D and triangle in 3D), it can be called Frenet Element Method. The average surface tension force is:

$$\bar{\mathbf{f}} = \frac{\sigma}{S} \int_S \kappa \mathbf{n} dS = \frac{\sigma}{S} \oint_{\partial S} \mathbf{t} \wedge \mathbf{n} dl \tag{2}$$

with $\wedge$ the cross product, S the area of the element, ∂S its perimeter, $\mathbf{t}$ and $\mathbf{n}$ the unit tangent and normal vectors at the edge. The average force is approximated by:

$$\bar{\mathbf{f}} \approx \frac{\sigma}{S} \sum_{i=1}^{3} (\mathbf{t_{0i}} \wedge \mathbf{n_{0i}}) L_{0i} \tag{3}$$

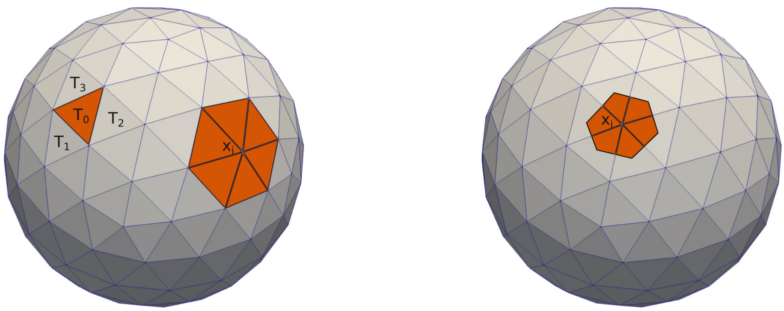

(a) Frenet element and vertex stencils (b) Standard Meyer stencil

Fig. 1. Areas on which are applied the average force for the frenet element and vertex methods (a) and the Standard Meyer method (b).

where $\bullet_{0i}$ refers to the parameters at the edge shared by elements T_0 and T_i. For an analytical surface, it is simple to get the tangent and the normal vector at the edge. This is more problematic for the approximated surface. To mimic the continuous formulation in the 3D discrete case, the normal vector to the edge shared by the elements T_0 and T_1 is approximated by:

$$\mathbf{n_{01}} = \frac{S_1\mathbf{n}_0 + S_0\mathbf{n}_1}{\|S_1\mathbf{n}_0 + S_0\mathbf{n}_1\|} \tag{4}$$

Instead of computing the mean values of the curvature and normal vector on the element, an average value centered around a vertex $\mathbf{x_i}$ can be preferred, the so called Frenet Vertex Method. The resulting surface tension force, constructed on the elements sharing the same vertex $\mathbf{x_i}$, consists in a linear combination of the average force on each element, using the Frenet Element Method:

$$\mathbf{F}(\mathbf{x_i}) = \sum_{j=1}^{\mathcal{N}_i} S_j\bar{\mathbf{f}}_j \quad \text{and} \quad \overline{\kappa\mathbf{n}} = \frac{\mathbf{F}(\mathbf{x_i})}{\sigma\sum_{j=1}^{\mathcal{N}_i} S_j} \tag{5}$$

3 Simulations and Results

The aforementioned methods are compared and their accuracy estimated on an analytical surface [6], where the exact curvature and normal vector are computed [5]. The following analytical surface is considered (see Fig. 2):

$$f(u, v) = \sin(5u)\sin(5v) \quad \text{with} \quad (u, v) \in [-\frac{\pi}{5}, \frac{\pi}{5}] \times [-\frac{\pi}{5}, \frac{\pi}{5}] \tag{6}$$

Its discrete approximation results in a projection of a planar mesh, for which the size and the shape of the elements are controlled. Let $\mathbf{x} = \big(x_1, x_2, 0\big)$ be a vertex of an initial planar mesh of equilateral triangles, the edges size of which

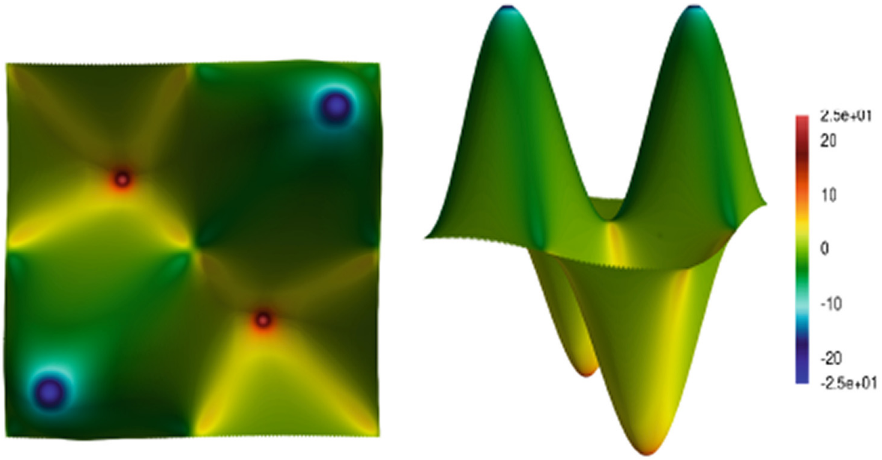

Fig. 2. Top view (left) and side view (right) of the mean curvature κ for the analytical surface $f(u, v)$ (Eq. 6).

is d. From this initial planar mesh, random disturbances are introduced: $\tilde{\mathbf{x}} = \mathbf{x} + r \times p \times d \times \big(\cos 2\pi\theta, \sin 2\pi\theta, 0\big)$, where p is the maximum magnitude of the perturbation ($0 \leq p < 0.5$), and (r, θ) is a couple of random numbers drawn from a standard uniform distribution. To evaluate the accuracy of the approximations, the following measure is defined:

$$\mathrm{Err}_2^{\mathrm{rel}}(\bullet) = \sqrt{\frac{\sum_{j=1}^{N} \| \bullet_j - \bullet_j^{ref} \|^2}{\sum_{j=1}^{N} \| \bullet_j^{ref} \|^2}} \tag{7}$$

where $\| \bullet \|$ is the absolute-value for a scalar number, or the Euclidean norm for a vector, N denotes the number of vertices (Meyer approach and Frenet Vertex Method) or elements (Frenet Element Method). The notation $\bullet_j^{ref}$ stands for the average force direction $\mathbf{n}_j^{ref}$ or intensity κ_j^{ref} on the surface $\mathcal{S}$, which corresponds to, either the element j, or the stencil surrounding the vertex $\mathbf{x}_j$:

$$\mathbf{n}_j^{ref} = \frac{\bar{\mathbf{F}}}{\|\bar{\mathbf{F}}\|}, \qquad \kappa_j^{ref} = \frac{\|\bar{\mathbf{F}}\|}{\sigma}, \quad \text{with} \quad \bar{\mathbf{F}} = \frac{\sigma}{\mathcal{S}} \int_{\mathcal{S}} \kappa \mathbf{n} ds \tag{8}$$

The convergence of the approximation is studied as a function of the dimensionless mesh size $d \times \max_j(\kappa_j^{ref})$, which represents the size of the triangles used for describing the maximum curvature. First, no perturbation is applied on the planar equilateral mesh ($p = 0$). The numerical errors reported in Table 1 indicate that the best methods which stand out are the Standard Meyer Method,

Table 1. Comparative and convergence study on κ, $p = 0$

$d \times \max(\kappa)$	Std Meyer		Bar Meyer		Frenet vertex		Frenet element	
	$\mathrm{Err}_2^{\mathrm{rel}}(\kappa)$	*Order*	$\mathrm{Err}_2^{\mathrm{rel}}(\kappa)$	*Order*	$\mathrm{Err}_2^{\mathrm{rel}}(\kappa)$	*Order*	$\mathrm{Err}_2^{\mathrm{rel}}(\kappa)$	*Order*
7.80E–01	2.04E–02		3.27E–02		1.98E–02		9.95E–02	
3.90E–01	6.20E–03	1.72	1.86E–02	0.81	7.20E–03	1.46	5.33E–02	0.90
1.95E–01	1.82E–03	1.77	1.42E–02	0.39	3.05E–03	1.24	2.72E–02	0.97
9.75E–02	5.38E–04	1.76	9.04E–03	0.66	1.13E–03	1.43	1.42E–02	0.94
4.87E–02	1.65E–04	1.71	6.75E–03	0.42	5.36E–04	1.08	7.22E–03	0.97
2.44E–02	5.31E–05	1.63	4.68E–03	0.53	2.07E–04	1.37	3.61E–03	1.00

Table 2. Comparative and convergence study on κ, $p = 0.05$

$d \times \max(\kappa)$	Std Meyer		Bar Meyer		Frenet vertex		Frenet element	
	$\mathrm{Err}_2^{\mathrm{rel}}(\kappa)$	*Order*	$\mathrm{Err}_2^{\mathrm{rel}}(\kappa)$	*Order*	$\mathrm{Err}_2^{\mathrm{rel}}(\kappa)$	*Order*	$\mathrm{Err}_2^{\mathrm{rel}}(\kappa)$	*Order*
7.80E–01	2.38E–02		3.39E–02		2.04E–02		1.02E–01	
3.90E–01	1.39E–02	0.78	2.34E–02	0.54	8.99E–03	1.18	5.90E–02	0.79
1.95E–01	1.24E–02	0.16	2.05E–02	0.19	5.90E–03	0.61	3.77E–02	0.65
9.75E–02	1.24E–02	0.00	2.00E–02	0.04	5.48E–03	0.11	3.03E–02	0.31
4.87E–02	1.24E–02	0.00	1.98E–02	0.01	5.44E–03	0.01	2.80E–02	0.11
2.44E–02	1.24E–02	0.00	1.98E–02	0.00	5.42E–03	0.00	2.74E–02	0.03

Table 3. Comparative and convergence study on $\mathbf{n}$, $p = 0.2$

$d \times \max(\kappa)$	Std Meyer		Bar Meyer		Frenet vertex		Frenet element	
	$\mathrm{Err}_2^{\mathrm{rel}}(n)$	*Order*	$\mathrm{Err}_2^{\mathrm{rel}}(n)$	*Order*	$\mathrm{Err}_2^{\mathrm{rel}}(n)$	*Order*	$\mathrm{Err}_2^{\mathrm{rel}}(n)$	*Order*
7.80E–01	1.23E–01		1.23E–01		1.56E–01		8.78E–02	
3.90E–01	5.23E–02	1.23	5.23E–02	1.23	6.39E–02	1.29	5.46E–02	0.69
1.95E–01	1.41E–02	1.90	1.40E–02	1.90	1.11E–02	2.52	2.72E–02	1.00
9.75E–02	3.93E–03	1.84	3.89E–03	1.85	2.83E–03	1.97	1.32E–02	1.04
4.87E–02	1.12E–03	1.82	1.08E–03	1.85	1.20E–03	1.24	6.75E–03	0.97
2.44E–02	3.53E–04	1.66	3.30E–04	1.71	5.08E–04	1.24	3.37E–03	1.00

followed by the Frenet Vertex one. From now on, random perturbations are introduced in the aforementioned planar mesh, and 100 simulations are performed to get the mean statistical values. As shown in Table 2 for small disturbances ($p = 0.05$), all methods saturate when refining the mesh. This saturation is all the more high as the magnitude p of the perturbations increases. Indeed, for $p = 0.2$ and $d \times \max_j(\kappa_j^{ref}) = 2.44 \times 10^{-2}$, the relative curvature errors for the Standard Meyer and the Frenet Vertex Methods are 4 times larger, with respectively $\mathrm{Err}_2^{\mathrm{rel}}(\kappa) = 4.96 \times 10^{-2}$ and $\mathrm{Err}_2^{\mathrm{rel}}(\kappa) = 2.35 \times 10^{-2}$. Concerning the normal vector approximation $\mathbf{n}$, even for large perturbations ($p = 0.2$), the methods converge, with at least a 1^{st} order accuracy (Table 3). However, despite the convergence of the unit normal vector, the saturation of the curvature prevents the convergence of the surface tension force.

4 Remarks and Conclusion

Getting the surface tension force, the mean curvature and the normal vector at the interface of multiphase flows is not as straightforward as in 2D, where the usual methods give good results, both in terms of errors and accuracy [9]. The tests conducted in this paper show that, without random perturbation, the Standard Meyer and the Frenet Vertex Methods stand out and have a good accuracy. It is worth to point out that, after projection onto the surface, the triangles are not equilateral anymore. However, the surface mesh still varies smoothly, since the analytical function is regular enough. In contrast, the addition of disturbances definitely breaks this regularity, preventing the convergence of the curvature (and the surface tension force). In the framework of multiphase flows approximated by 3D front-tracking methods, the mesh quality is difficult to manage because of the complexity of the dynamics. Therefore, despite relatively small errors, applying the different methods is questionable due to their lack of convergence.

References

1. Brackbill, J., Kothe, D., Zemach, C.: A continuum method for modeling surface tension. J. Comput. Phys. **100**(2), 335–354 (1992)
2. Compere, G., Marchandise, E., Remacle, J.F.: Transient adaptivity applied to two-phase incompressible flows. J. Comput. Phys. **227**(3), 1923–1942 (2008)
3. Delhaye, J.: Jump conditions and entropy sources in two-phase systems. Local instant formulation. Int. J. Multiph. Flow **1**(3), 395–409 (1974)
4. Essadki, M.: Contribution to a unified Eulerian modeling of fuel injection: from dense liquid to polydisperse evaporating spray. Ph.D. thesis, Universite Paris-Saclay (2018)
5. Goldman, R.: Curvature formulas for implicit curves and surfaces. Comput. Aided Geometr. Design **22**, 632–658 (2005)
6. Li, X., Xu, G., Zhang, Y.J.: Localized discrete laplacebeltrami operator over triangular mesh. Comput. Aided Geometr. Design **39**, 67–82 (2015)
7. Meyer, M., Desbrun, M., Schroder, P., Barr, A.H.: Discrete differential-geometry operators for triangulated 2-manifolds. In: Hege, H.C., Polthier, K. (eds.) Visualization and Mathematics III, pp. 35–57. Springer, Heidelberg (2003)
8. Shin, S., Juric, D.: Modeling three-dimensional multiphase flow using a level contour reconstruction method for front tracking without connectivity. J. Comput. Phys. **180**(2), 427–470 (2002)
9. Tavares, M., Koffi-Bi, D.A., Chénier, E., Vincent, S.: A second order conservative front-tracking method with an original marker advection method based on jump relations. Commun. Comput. Phys. (2020, to be published)
10. Tryggvason, G., Scardovelli, R., Zaleski, S.: Direct Numerical Simulations of Gas-Liquid Multiphase Flows, 1st edn. Cambridge University Press, Cambridge (2011)